Journal of Computational Mathematics, Vol.25, No.4, 2007, 385–407.

SURFACE FINITE ELEMENTS FOR PARABOLIC EQUATIONS [*1)]

G. Dziuk
(*Abteilung für Angewandte Mathematik, University of Freiburg, Hermann-Herder-Straße 10 D–79104, Freiburg i. Br., Germany*
Email: gerd.dziuk@mathematik.uni-freiburg.de)

C. M. Elliott
(*Department of Mathematics, University of Sussex, Falmer Brighton BN1 9RF, United Kingdom*
Email: c.m.elliott@sussex.ac.uk)

Abstract

In this article we define a surface finite element method (SFEM) for the numerical solution of parabolic partial differential equations on hypersurfaces Γ in $\mathbb{R}^{n+1}$. The key idea is based on the approximation of Γ by a polyhedral surface Γ_h consisting of a union of simplices (triangles for $n = 2$, intervals for $n = 1$) with vertices on Γ. A finite element space of functions is then defined by taking the continuous functions on Γ_h which are linear affine on each simplex of the polygonal surface. We use surface gradients to define weak forms of elliptic operators and naturally generate weak formulations of elliptic and parabolic equations on Γ. Our finite element method is applied to weak forms of the equations. The computation of the mass and element stiffness matrices are simple and straightforward. We give an example of error bounds in the case of semi-discretization in space for a fourth order linear problem. Numerical experiments are described for several linear and nonlinear partial differential equations. In particular the power of the method is demonstrated by employing it to solve highly nonlinear second and fourth order problems such as surface Allen-Cahn and Cahn-Hilliard equations and surface level set equations for geodesic mean curvature flow.

Mathematics subject classification: 65M60, 65M30, 65M12, 65Z05, 58J35, 53A05, 74S05, 80M10, 76M10.
Key words: Surface partial differential equations, Surface finite element method, Geodesic curvature, Triangulated surface.

1. Introduction

Partial differential equations on surfaces occur in many applications. For example, traditionally they arise naturally in fluid dynamics and material science and more recently in the mathematics of images. In this paper we propose a mathematical approach to the formulation and finite element approximation of parabolic equations on a surface in $\mathbb{R}^{n+1}$ $(n = 1, 2)$. We give examples of linear and nonlinear equations. In particular we show how surface level set and phase field models can be used to compute the motion of curves on surfaces.

[*] Received September 25, 2006; final revised February 8, 2007; accepted March 3, 2007.
[1)] The work was supported by the Deutsche Forschungsgemeinschaft via DFG-Forschergruppe *Nonlinear partial differential equations: Theoretical and numerical analysis* and by the UK EPSRC via the Mathematics Research Network: *Computation and Numerical analysis for Multiscale and Multiphysics Modelling.* Part of this work was done during a stay of the first author at the ICM at the University of Warsaw supported by the *Alexander von Humboldt Honorary Fellowship 2005* granted by the Foundation for Polish Science.

1.1. The diffusion equation

Conservation on a hypersurface Γ of a scalar u with a diffusive flux $-\mathcal{D}\nabla_\Gamma w$, where $\mathcal{D}$ is the diffusivity tensor and w is a scalar, leads to the diffusion equation

$$u_t - \nabla_\Gamma \cdot (\mathcal{D}\nabla_\Gamma w) = 0 \tag{1.1}$$

on Γ. Here ∇_Γ is the tangential or surface gradient. If $\partial\Gamma$ is empty then the equation does not need a boundary condition. Otherwise we can impose Dirichlet or no flux boundary conditions on $\partial\Gamma$. Choosing various constitutive relations to define the relationship between the flux and u leads to a variety of second and fourth order linear and nonlinear parabolic equations. For example the constitutive relations $w = u$ and $w = -\Delta_\Gamma u$ lead to linear second and fourth order diffusion equations.

1.2. The finite element method

In this paper we propose a finite element approximation based on the variational form

$$\int_\Gamma u_t \varphi + \int_\Gamma \mathcal{D}\nabla_\Gamma w \cdot \nabla_\Gamma \varphi = 0 \tag{1.2}$$

where φ is an arbitrary test function defined on the surface Γ in $\mathbb{R}^3$ with $\partial\Gamma$ empty. This provides the basis of our surface finite element method (SFEM) which is applicable to arbitrary n–dimensional hypersurfaces in $\mathbb{R}^{n+1}$ (curves in $\mathbb{R}^2$) with or without boundary. Indeed this is the extension of the method from [10] for the Laplace-Beltrami equation, which was extended to linear second order diffusion equations on moving surfaces in [12]. We focus our description on the case $n = 2$ but observe that the approach is directly applicable to $n = 1$.

The principal idea is to use a polyhedral approximation of Γ based on a triangulated surface. It follows that a quite natural local piecewise linear parametrization of the surface is employed rather than a global one. The finite element space is then the space of continuous piecewise linear functions on the triangulated surface. The implementation is thus rather similar to that for solving the diffusion equation on flat stationary domains. For example, for $w = u$, the backward Euler time discretization leads to the SFEM scheme

$$\frac{1}{\tau}\left(\mathcal{M}\alpha^{m+1} - \mathcal{M}\alpha^m\right) + \mathcal{S}\alpha^{m+1} = 0$$

where $\mathcal{M}$ and $\mathcal{S}$ are the surface mass and stiffness matrices and α^m is the vector of nodal values for the approximation of u at time t^m. Here, τ denotes the time step size. Observe that this approach to evolutionary surface partial differential equations was used in [11] to evolve a surface by mean curvature flow. See also [5].

1.3. Level set or implicit surface approach

An alternative approach to our method based on the use of (1.2) is to embed the surface in a family of level set surfaces [1, 3, 4, 13, 14, 21, 30]. This Eulerian approach can be discretized on a Cartesian grid in $\mathbb{R}^{n+1}$ and has the usual advantages and disadvantages of level set methods. Equations on surfaces also arise in phase field models [7, 19, 25].

1.4. Applications

Models involving partial differential equations on surfaces arise in many areas including material science, bio-physics, fluid mechanics and image processing. For example, phase formation of surface alloying by spinodal decomposition resulting in two dimensional structures has been modelled by the Cahn-Hilliard equation on surfaces, [8]. See also [26, 27] for studies of the Allen-Cahn and Cahn-Hilliard equations in the context of phase ordering on surfaces. Other examples in the physical sciences include diffusion induced grain boundary motion [7, 19, 23] and the Ginzburg-Landau model for superconductivity [9]. In image processing we mention geodesic flow of curves on surfaces and active contours for segmentation on surfaces, [22, 24].

1.5. Outline of paper

The layout of the paper is as follows. We begin in Section 2 by defining notation and essential concepts from elementary differential geometry necessary to describe the problem and numerical method. Several linear and nonlinear partial differential equations of second and fourth order are described in Section 3 together with a number of computational results. In Section 4 the finite element method is defined and some preliminary approximation results are shown. Error bounds for the semi-discretization in space are proved in Section 5. Implementation issues are discussed in Section 6.

2. Basic Notation and Surface Derivatives

Let Γ be a compact smooth connected and oriented hypersurface in $\mathbb{R}^{n+1}$ $(n = 1, 2)$. In order to formulate the model it is convenient to use a level set description of Γ.

We assume the existence of a smooth level set function $d = d(x)$, $x \in \mathbb{R}^{n+1}$, so that

$$\Gamma = \{x \in \mathcal{N} | \, d(x) = 0\},$$

where $\mathcal{N}$ is an open subset of $\mathbb{R}^{n+1}$ in which $\nabla d \neq 0$ and chosen so that

$$d \in C^2(\mathcal{N}).$$

The orientation of Γ is fixed by taking the normal ν to Γ to be in the direction of increasing d. Hence we define a normal vector field by

$$\nu(x) = \frac{\nabla d(x)}{|\nabla d(x)|}.$$

Throughout this paper we denote by $\mathcal{P}(x)$ the projection at x onto the tangent space of Γ with i, j element

$$\mathcal{P}(x)_{ij} = \delta_{ij} - \nu(x)_i \nu(x)_j. \tag{2.1}$$

Observe that a possible choice for d is a signed distance function and in that case $|\nabla d| = 1$ on $\mathcal{N}$. For later use we mention that $\mathcal{N}$ can be chosen such that for every $x \in \mathcal{N}$ there exists a unique $a(x) \in \Gamma$ such that

$$x = a(x) + d(x)\nu(a(x)), \tag{2.2}$$

where d denotes the signed distance function to Γ.

For any function η defined on an open subset $\mathcal{N}$ of $\mathbb{R}^{n+1}$ containing Γ we define its tangential gradient on Γ by

$$\nabla_\Gamma \eta = \nabla \eta - \nabla \eta \cdot \nu \, \nu = \mathcal{P} \nabla \eta,$$

where, for x and y in $\mathbb{R}^{n+1}$, $x \cdot y$ denotes the usual scalar product and $\nabla \eta$ denotes the usual gradient on $\mathbb{R}^{n+1}$. The tangential gradient $\nabla_\Gamma \eta$ only depends on the values of η restricted to Γ and $\nabla_\Gamma \eta \cdot \nu = 0$. The components of the tangential gradient will be denoted by

$$\nabla_\Gamma \eta = \left(\underline{D}_1 \eta, \ldots, \underline{D}_{n+1} \eta \right).$$

The Laplace-Beltrami operator on Γ is defined as the tangential divergence of the tangential gradient:

$$\Delta_\Gamma \eta = \nabla_\Gamma \cdot \nabla_\Gamma \eta = \sum_{i=1}^{n+1} \underline{D}_i \underline{D}_i \eta.$$

Let Γ have a boundary $\partial \Gamma$ whose intrinsic unit outer normal (conormal), tangential to Γ, is denoted by μ. Then for $i = 1, 2, \ldots, n+1$, the formula for integration on Γ is, see [15],

$$\int_\Gamma \underline{D}_i \eta = - \int_\Gamma \eta H \nu_i + \int_{\partial \Gamma} \eta \mu_i, \tag{2.3}$$

yielding the divergence theorem for $\xi = (\xi_1, \xi_2, \ldots, \xi_{n+1})$,

$$\int_{\partial \Gamma} \xi \cdot \mu = \int_\Gamma \nabla_\Gamma \cdot \xi + \int_\Gamma \xi \cdot \nu H \tag{2.4}$$

where H denotes the mean curvature of Γ with respect to ν, which is given by

$$H = -\nabla_\Gamma \cdot \nu. \tag{2.5}$$

The orientation is such that for a sphere $\Gamma = \{x \in \mathbb{R}^{n+1} | \, |x - x_0| = R\}$ and the choice $d(x) = R - |x - x_0|$ the normal is pointing into the ball $B_R(x_0) = \{x \in \mathbb{R}^{n+1} | \, |x - x_0| < R\}$ and the mean curvature of Γ is given by $H = n/R$. Note that H is the sum of the principle curvatures rather than the arithmetic mean and hence differs from the common definition by a factor n. The mean curvature vector $H\nu$ is invariant with respect to the choice of the sign of d.

Green's formula on the surface Γ is

$$\int_\Gamma \nabla_\Gamma \xi \cdot \nabla_\Gamma \eta = \int_{\partial \Gamma} \xi \nabla_\Gamma \eta \cdot \mu - \int_\Gamma \xi \Delta_\Gamma \eta. \tag{2.6}$$

If Γ is closed then $\partial \Gamma$ is empty and the boundary terms in equations (2.3),(2.4), and (2.6) do not appear. For these facts about tangential derivatives we refer to [20], pp. 389-391. Note that, in general, higher order tangential derivatives do not commute.

We shall use Sobolev spaces on surfaces Γ. For a given surface Γ we define

$$H^1(\Gamma) = \{\eta \in L^2(\Gamma) \mid \nabla_\Gamma \eta \in L^2(\Gamma)^{n+1}\}$$

and, if $\partial \Gamma \neq \emptyset$,

$$H_0^1(\Gamma) = \{\eta \in H^1(\Gamma) \mid \eta = 0 \text{ on } \partial \Gamma\}.$$

For smooth enough Γ we analogously define the Sobolev spaces $H^k(\Gamma)$ for $k \in \mathbb{N}$. See [29] for additional information.

3. Parabolic Equations on Surfaces

3.1. Conservation and diffusion on a surface

Let $u = u(x,t)$ $(x \in \Gamma,\ t \in [0,T])$ be the density of a scalar quantity on Γ (for example mass per unit area if $n = 2$ or mass per unit length if $n = 1$). The basic conservation law we wish to consider can be formulated for an arbitrary portion $\mathcal{M}$ of Γ using a surface flux q. The law is that, for every $\mathcal{M}$,

$$\frac{d}{dt}\int_{\mathcal{M}} u = -\int_{\partial\mathcal{M}} q \cdot \mu, \tag{3.1}$$

where $\partial\mathcal{M}$ is the boundary of $\mathcal{M}$ (a curve if $n = 2$ and the end points of a curve if $n = 1$) and μ is the conormal on $\partial\mathcal{M}$. Thus μ is the unit normal to $\partial\mathcal{M}$ pointing out of $\mathcal{M}$ and tangential to Γ. Observe that components of q normal to $\mathcal{M}$ do not contribute to the flux, so, without loss of generality, we assume that q is a tangent vector.

Using the divergence theorem (2.4) and the fact that q is a tangential vector we obtain

$$\int_{\partial\mathcal{M}} q \cdot \mu = \int_{\mathcal{M}} \nabla_\Gamma \cdot q + \int_{\mathcal{M}} q \cdot \nu H = \int_{\mathcal{M}} \nabla_\Gamma \cdot q,$$

so that

$$\int_{\mathcal{M}} (u_t + \nabla_\Gamma \cdot q) = 0,$$

which implies the pointwise conservation law

$$u_t + \nabla_\Gamma \cdot q = 0 \quad \text{on} \quad \Gamma. \tag{3.2}$$

We take q to be the diffusive flux

$$q = -\mathcal{D}\nabla_\Gamma w, \tag{3.3}$$

where $\mathcal{D} \geq 0$ is a symmetric mobility tensor with the property that it maps the tangent space into itself at every point of Γ, i.e.,

$$\mathcal{D}\nu^\perp \cdot \nu = 0 \tag{3.4}$$

for every tangent vector $\nu^\perp$. This leads to the equation

$$u_t - \nabla_\Gamma \cdot (\mathcal{D}\nabla_\Gamma w) = 0 \quad \text{on} \quad \Gamma. \tag{3.5}$$

Since $\partial\Gamma = \emptyset$, i.e., the surface has no boundary, there is no need for boundary conditions. For example, this would be the case if Γ is the bounding surface of a domain.

Remark 3.1. If $\partial\Gamma$ is non-empty then we may impose the homogeneous Dirichlet boundary condition

$$u = 0 \ \text{ on } \ \partial\Gamma, \tag{3.6}$$

or impose the no flux condition

$$\mathcal{D}\nabla_\Gamma w \cdot \mu = 0 \quad \text{on} \quad \partial\Gamma. \tag{3.7}$$

The variational form (1.2) then is an easy consequence of (1.1). We multiply equation (1.1) by an arbitrary test function $\varphi \in H^1(\Gamma)$ and integrate over Γ. We then obtain using (2.4):

$$\int_\Gamma u_t\varphi + \int_\Gamma \mathcal{D}\nabla_\Gamma w \cdot \nabla_\Gamma \varphi = 0. \tag{3.8}$$

Here and in all subsequent equations we have to impose an initial condition $u(\cdot, 0) = u_0$. In the following we will not mention this condition when it is obviously required.

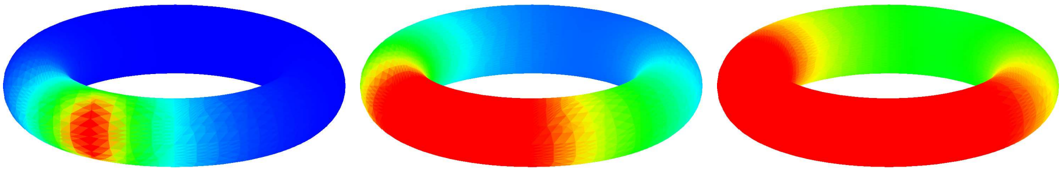

Fig. 3.1. Heating up a torus. Solution at times 0.06934, 0.3467 and 0.6934.

Remark 3.2. Note that for arbitrary $\mathcal{D}$ this weak equation implies

$$u_t - \nabla_\Gamma \cdot (\mathcal{P}\mathcal{D}\nabla_\Gamma w) = 0 \quad \text{on} \quad \Gamma. \tag{3.9}$$

Also, in general, constant coefficient mobility tensors $\mathcal{D}$ will not satisfy assumption (3.4) and $\mathcal{P}$ will not be constant coefficient.

Remark 3.3 (Conservation) Taking $\varphi = 1$ in (3.8) yields the conservation equation

$$\frac{d}{dt}\int_\Gamma u = 0.$$

Example 3.4 (Linear diffusion) Setting $w = u$ and $\mathcal{D} = \mathcal{I}$, where $\mathcal{I}$ is the identity tensor, we find the heat equation on surfaces

$$u_t = \Delta_\Gamma u. \tag{3.10}$$

Clearly this can be generalized to the inhomogeneous equation

$$u_t - \Delta_\Gamma u = f. \tag{3.11}$$

In Fig. 3.1 we display the solution at three successive times of (3.11) on the torus

$$\Gamma = \left\{ x \in \mathbb{R}^3 | \, (\sqrt{x_1^2 + x_2^2} - 1)^2 + x_3^2 = \frac{1}{16} \right\} \tag{3.12}$$

with the right hand side being a regularized version of the characteristic function

$$f(x,t) = 100\,\chi_G(x), \quad x \in \Gamma,$$

with $G = \{x \in \Gamma |\, |x - (0,1,0)| < 0.25\}$ and with initial value $u_0 = 0$.

For the choice $\mathcal{D} = \mathcal{A} = (a_{ij}(x,t))_{i,j=1,\dots,n+1}$ with a symmetric matrix $\mathcal{A}$ which satisfies (3.4) and is positive definite on the space orthogonal to ν we obtain the linear parabolic PDE

$$u_t = \sum_{i,j=1}^{n+1} \underline{D}_i \left(a_{ij} \underline{D}_j u \right). \tag{3.13}$$

Example 3.5 (Nonlinear diffusion) Setting

$$w = f(u) \quad \text{and} \quad \mathcal{D} = m(u)\mathcal{I}$$

for given continuous functions $f(\cdot)$ and $m(\cdot)$ we find the nonlinear diffusion equation

$$u_t = \nabla_\Gamma \cdot (a(u)\nabla_\Gamma u) \tag{3.14}$$

where $a(u) = m(u)f'(u)$, and $a(\cdot)$ is positive if $f(\cdot)$ is monotone increasing and $m(\cdot)$ is positive. Clearly one recovers linear diffusion and the porous medium equation by suitable choices.

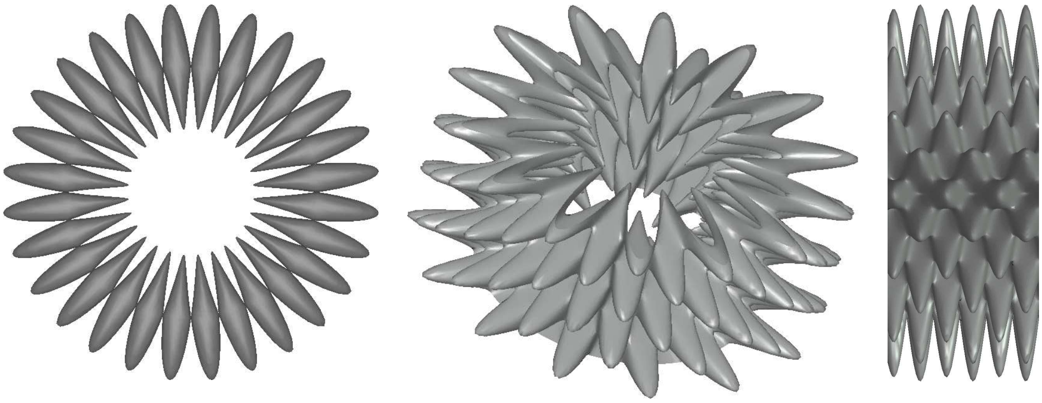

Fig. 3.2. Strongly deformed cylinder: Views from x_3-axis, tilted axis, and x_1-axis.

Example 3.6 (Parabolic surface p–Laplace equation) Setting $w = u$ and, for $1 < p$,

$$\mathcal{D} = |\nabla_\Gamma u|^{p-2}\mathcal{I}$$

yields the following parabolic surface p–Laplace equation

$$u_t = \nabla_\Gamma \cdot \big(|\nabla_\Gamma u|^{p-2}\nabla_\Gamma u\big) \tag{3.15}$$

which is $L^2(\Gamma)$-gradient flow for the energy

$$E_p(u) = \frac{1}{p}\int_\Gamma |\nabla_\Gamma u|^p. \tag{3.16}$$

Example 3.7 (Total variation flow) Setting $w = u$ and taking

$$\mathcal{D} = |\nabla_\Gamma u|^{-1}\mathcal{I}$$

leads formally to the surface total variation flow

$$u_t = \nabla_\Gamma \cdot \frac{\nabla_\Gamma u}{|\nabla_\Gamma u|}. \tag{3.17}$$

Example 3.8 (Fourth order linear diffusion) The choice

$$w = -\Delta_\Gamma u \tag{3.18}$$

leads to the fourth order linear diffusion equation

$$u_t = -\nabla_\Gamma \cdot (\mathcal{D}\nabla_\Gamma \Delta_\Gamma u)\,. \tag{3.19}$$

Example 3.9 (Surface Cahn-Hilliard equation) Setting

$$w = -\epsilon\Delta_\Gamma u + \frac{1}{\epsilon}\Psi'(u), \tag{3.20}$$

where $\Psi : \mathbb{R} \to \mathbb{R}$ typically is a double well potential,

$$\Psi(u) = \frac{1}{4}(1-u^2)^2, \tag{3.21}$$

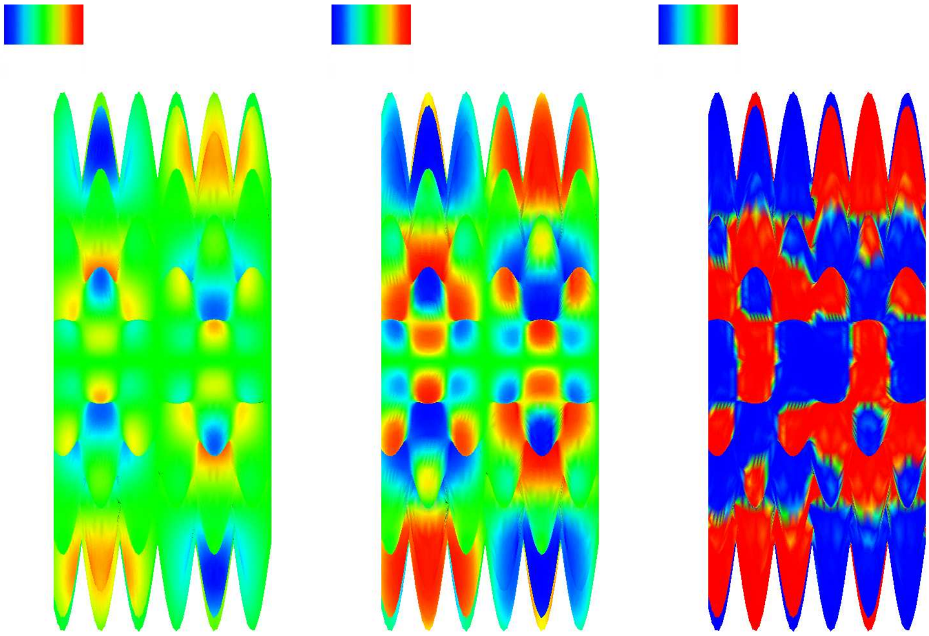

Fig. 3.3. Solution of the Cahn-Hilliard equation on the surface from Figure 3.2. View from the x_1-axis with x_3-axis pointing to the right. The colours represent the magnitude of the solution between -1 and 1. Times from left to right: $t = 0.0, 0.012047, 0.11130$.

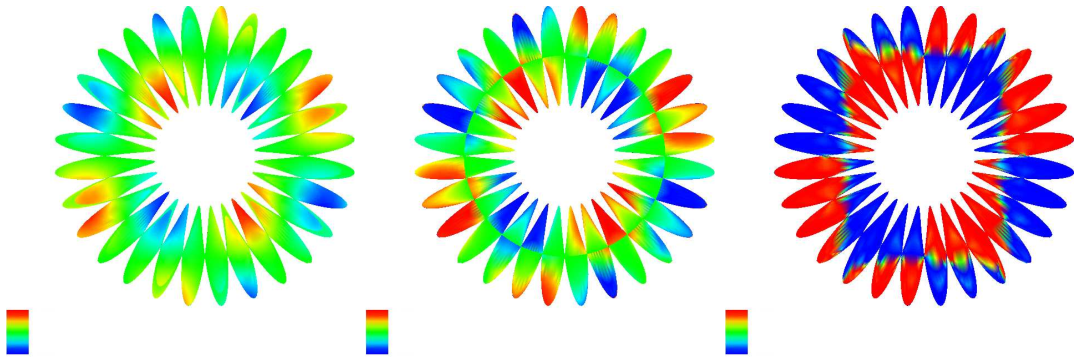

Fig. 3.4. The same situation as in Fig. 3.3 seen from the x_3-axis.

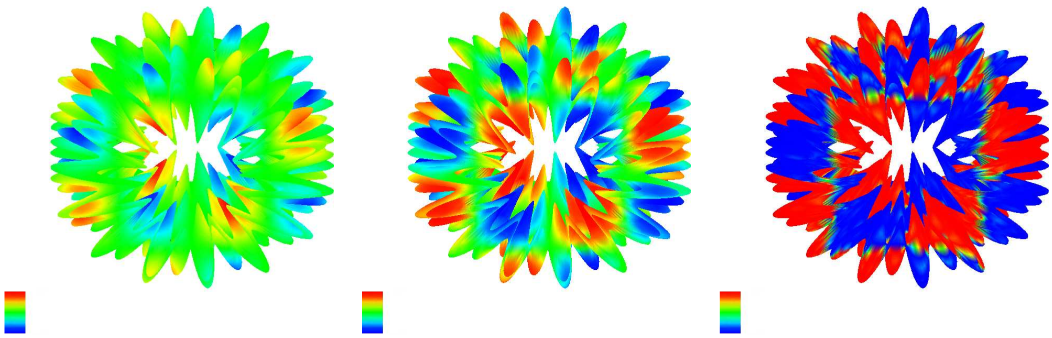

Fig. 3.5. The same situation as in Fig. 3.3: tilted view.

leads to the fourth order Cahn-Hilliard equation

$$u_t = -\nabla_\Gamma \cdot \left(\mathcal{D} \nabla_\Gamma (\epsilon \Delta_\Gamma u - \frac{1}{\epsilon} \Psi'(u)) \right). \tag{3.22}$$

Using second order splitting as introduced in [17] we formulate the problem as a system of second order equations in space. We solved the Cahn-Hilliard equation for $\mathcal{D} = \mathcal{I}$ on a strongly deformed surface (see Fig. 3.2). The topology of the surface is cylindrical: $\Gamma = F(\Gamma_0)$, where

$$F(x_1, x_2, x_3) = f(x_1, x_2, x_3)(x_1, x_2, 0) + (0, 0, x_3)$$

with $f(x) = 1 + 0.5 \sin(14\varphi) \sin(15x_3)$ and φ is the polar angle in the x_1, x_2-plane. As reference surface we have chosen the cylinder $\Gamma_0 = \{x \in \mathbb{R}^3 |\, x_1^2 + x_2^2 < 1, 0 < x_3 < 1.2\}$. As initial value we have taken

$$u_0(x) = \sin(4x_1) \sin(3x_2) \sin(5x_3).$$

The grid contained $N = 24960$ nodes. We have used $\varepsilon = 0.01$. Colour maps of the solution are depicted in Figs. 3.3, 3.4 and 3.5.

3.2. Equations in non-conservation form

Here we formulate several time dependent equations on surfaces which are not in conservation form.

Example 3.10 (Surface Allen-Cahn equation) Consideration of the $L^2(\Gamma)$-gradient flow for the gradient energy functional

$$E(v) = \int_\Gamma \left(\frac{\epsilon}{2} |\nabla_\Gamma v|^2 + \frac{\Psi(v)}{\epsilon} \right), \tag{3.23}$$

($\epsilon > 0$) leads to

$$\epsilon u_t = \epsilon \Delta_\Gamma u - \frac{1}{\epsilon} \Psi'(u). \tag{3.24}$$

Here the potential (3.21) gives the classical Allen-Cahn equation on a surface Γ.

In Fig. 3.6 we show results of the numerical solution of the surface Allen-Cahn equation on the torus (3.12) with initial data

$$u_0(x) = \sin(3\pi x_3) \cos(3\varphi),$$

where φ denotes the polar angle in the x_1, x_2-plane. We observe the rapid evolution to a checkerboard pattern on the torus (first row). After some time this pattern is dissolved and the solution evolves to an interesting stationary solution (second row). It is interesting to observe that the red and blue regions are connected, so that there is just one diffuse interface which approximates a curve of zero geodesic curvature.

In Fig. 3.7 we show the typical decomposition effect of the Allen-Cahn equation on a deformed cylinder. Here the initial value u_0 was chosen to be a random distribution of matter on the surface.

Example 3.11 (Level set geodesic mean curvature flow) We formulate the level set equation

$$u_t = |\nabla_\Gamma u| \, \nabla_\Gamma \cdot \frac{\nabla_\Gamma u}{|\nabla_\Gamma u|}. \tag{3.25}$$

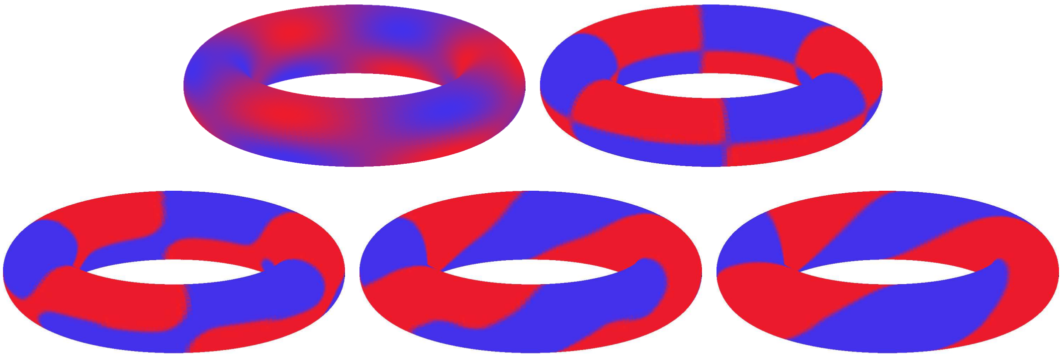

Fig. 3.6. Solution of the surface Allen-Cahn equation on a torus.

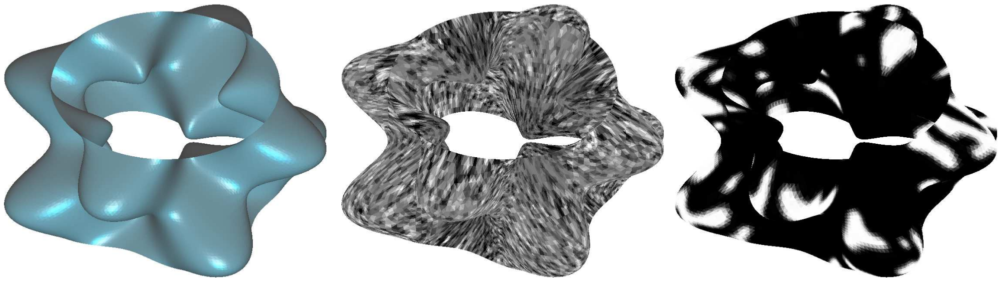

Fig. 3.7. Solution of the Allen-Cahn equation on a deformed cylinder (surface, initial distribution, distribution after some time).

For example, we have in mind the evolution, on the fixed surface Γ in $\mathbb{R}^3$, of a closed curve $\mathcal{C}(t)$ which is evolving in the "intrinsic" normal direction ν_g with a velocity V_g given by minus its geodesic curvature κ_g. The curve $\mathcal{C}(t)$ is given by the zero level set on Γ of $u(\cdot,t)$ and

$$\nu_g = \frac{\nabla_\Gamma u}{|\nabla_\Gamma u|}\,, \quad \kappa_g = \nabla_\Gamma \cdot \frac{\nabla_\Gamma u}{|\nabla_\Gamma u|}\,, \quad V_g = -\frac{u_t}{|\nabla_\Gamma u|}.$$

Fig. 3.8 shows how circles on a dumbbell shaped surface move under geodesic mean curvature flow. The surface Γ is given as $\Gamma = F(S^2)$ where $F(x) = (x_1, \eta(x)x_2, \eta(x)x_3)$ with

$$\eta(x) = \sqrt{1-x_1^2}\sqrt{1-0.8(1-x_1^2)^2}/\sqrt{x_2^2+x_3^2}$$

for $x \in S^2$. The initial function is $u_0(x) = x_1 - 0.25$. In Fig. 3.8 we display all the level lines $\{x \in \Gamma|\, u(x,t) = c\}$ for c between -1.05 and 1.25 with intervals of 0.2.

We observe that circles shrink and either move to the center of the dumbbell's neck or shrink to round points at the extreme ends of the dumbbell. Each of these possibilities is displayed in Fig. 3.9 for a single circle.

Finally in Fig. 3.10 we show the evolution of many level sets on the sphere. We see topology change of the level sets. In this computation we use the initial value

$$u_0(x) = \sin(5\pi(x_1 - 0.25))\sin(3\pi(x_3 + 0.25)).$$

In all these computations of geodesic curve shortening flow we regularized the equations by replacing $|\nabla_\Gamma u|$ by $\sqrt{\varepsilon^2 + |\nabla_\Gamma u|^2}$, and we have taken the parameter ε proportional to the grid size h.

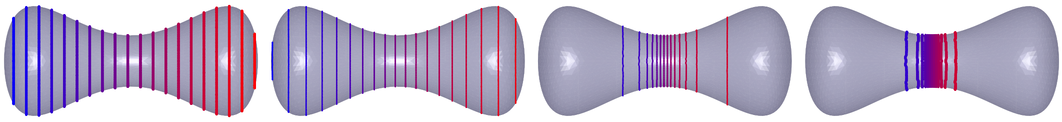

Fig. 3.8. Geodesic curve shortening flow on a dumbbell.

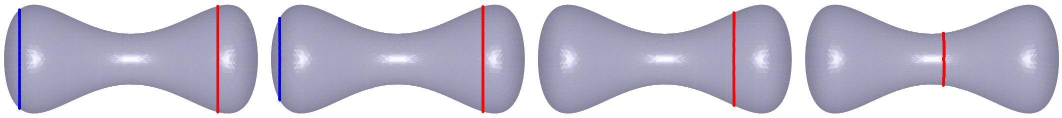

Fig. 3.9. Geodesic curve shortening flow for two circles on a dumbbell.

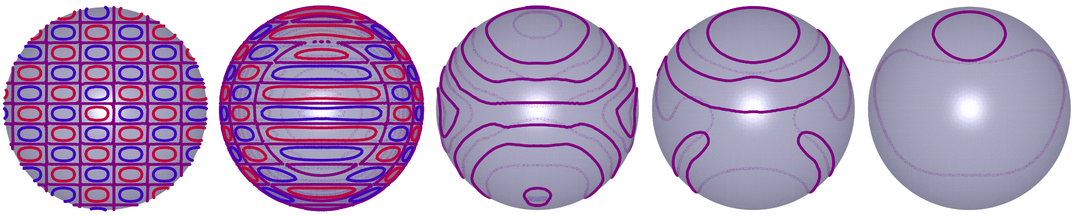

Fig. 3.10. Level set mean curvature flow on the sphere.

Example 3.12 (Level Set Surface Active Contours) We formulate the level set equation

$$u_t = |\nabla_\Gamma u| \nabla_\Gamma \cdot \left(f \frac{\nabla_\Gamma u}{|\nabla_\Gamma u|} \right) \tag{3.26}$$

where

$$f = \frac{1}{1 + |\nabla_\Gamma I_\sigma|^2}. \tag{3.27}$$

In (3.27), I_σ is a smoothed image which is essentially a characteristic function with sharp edges. The evolution of the zero level set curve $\mathcal{C}(t)$ is designed to detect the edge.

Example 3.13 (Anisotropic geodesic level set mean curvature flow) We formulate the level set equation for anisotropic mean curvature flow on the given surface Γ as

$$\mu(\nabla_\Gamma u) u_t = |\nabla_\Gamma u| \nabla_\Gamma \cdot D\gamma(\nabla_\Gamma u), \tag{3.28}$$

where $\gamma : \mathbb{R}^{n+1} \setminus \{0\} \to (0, \infty)$, $\gamma(0) = 0$, is an anisotropy function, smooth and positively homogeneous of degree one. Here $D\gamma$ denotes the gradient of γ. μ is a positive and 0-homogeneous function.

Example 3.14 (Level set geodesic surface diffusion) We formulate the level set equation

$$u_t = \nabla_\Gamma \cdot (|\nabla_\Gamma u| (\mathcal{I} - \nu_g \otimes \nu_g) \nabla_\Gamma w), \tag{3.29}$$

$$w = \nabla_\Gamma \cdot \frac{\nabla_\Gamma u}{|\nabla_\Gamma u|}. \tag{3.30}$$

For example, we have in mind the evolution, on the fixed surface Γ in $\mathbb{R}^3$, of a closed curve $\mathcal{C}(t)$ which is evolving in the "intrinsic" normal direction ν_g with a velocity V given by the geodesic Laplacian of the geodesic curvature κ_g. The curve $\mathcal{C}(t)$ is given by the zero level set on Γ of $u(\cdot, t)$.

Example 3.15 (Level set geodesic Willmore flow) We formulate the level set equation

$$u_t = -|\nabla_\Gamma u| \nabla_\Gamma \cdot \left(\frac{1}{|\nabla_\Gamma u|} (\mathcal{I} - \nu_g \otimes \nu_g) \nabla_\Gamma w \right) + \frac{1}{2} |\nabla_\Gamma u| \nabla_\Gamma \cdot \left(\frac{w^2}{|\nabla_\Gamma u|^2} \frac{\nabla_\Gamma u}{|\nabla_\Gamma u|} \right), \quad (3.31)$$

$$w = -|\nabla_\Gamma u| \, \nabla_\Gamma \cdot \frac{\nabla_\Gamma u}{|\nabla_\Gamma u|}. \quad (3.32)$$

Here the zero level set of u is the curve $\mathcal{C}(t)$ constrained to lie on Γ which evolves according to L^2 gradient flow for the energy

$$\mathcal{E}_{\mathcal{C}} = \frac{1}{2} \int_{\mathcal{C}} \kappa_g^2. \quad (3.33)$$

4. Finite Element Approximation

4.1. Finite elements on surfaces

The smooth surface Γ ($\partial\Gamma = \emptyset$) is approximated by a Lipschitz continuous surface $\Gamma_h \subset \mathcal{N}$ ($\partial\Gamma_h = \emptyset$). In particular for $n = 2$, $\Gamma_h = \cup_{e \in \mathcal{T}_h} e$ is a triangulated (and hence polyhedral) surface consisting of triangles e in $\mathcal{T}_h$ with maximum diameter being denoted by h and inner radius bounded below by ch with some $c > 0$. The vertices $\{X_j\}_{j=1}^N$ of the triangles are taken to sit on Γ so that Γ_h is an interpolation. Each edge of a triangle $e_1 \in \mathcal{T}_h$ is an edge of another triangle $e_2 \in \mathcal{T}_h$. Note that by (2.2) for every triangle $e \subset \Gamma_h$ there is a unique curved triangle $T = a(e) \subset \Gamma$. In order to avoid a global double covering (see [12]) we assume that,

$$\text{for each point } a \in \Gamma \text{ there is at most one point } x \in \Gamma_h \text{ with } a = a(x). \quad (4.1)$$

This implies that there is a bijective correspondence between the triangles on Γ_h and the induced curvilinear triangles on Γ.

For any continuous function η defined on the discrete surface Γ_h we may define an extension or lift onto Γ by

$$\eta^l(a) = \eta(x(a)), \quad a \in \Gamma, \quad (4.2)$$

where by (2.2) and our assumptions, $x(a)$ is defined as the unique solution of

$$x = a + d(x)\nu(a). \quad (4.3)$$

Furthermore we understand by $\eta^l(x)$ the constant extension from Γ in the normal direction $\nu(a)$. We denote by ν_h the normal to Γ_h which is constant on each element e. An application of the chain rule for differentiation gives

$$\nabla_{\Gamma_h} \eta = \mathcal{P}_h (\mathcal{I} - d\mathcal{H}) \nabla_\Gamma \eta^l(a(x)) \quad (4.4)$$

where $\mathcal{P}_h$ is the discrete projection

$$\mathcal{P}_{h,ij} = \delta_{ij} - \nu_{h,i}\nu_{h,j}$$

and $\mathcal{H}$ is the matrix of second derivatives of the distance function d with i, j element

$$\mathcal{H}_{i,j} = d_{x_i x_j}.$$

We have a finite element space

$$S_h = \left\{ \phi \in C^0(\Gamma_h) | \, \phi|_e \text{ is linear affine for each } e \in \mathcal{T}_h \right\} = \operatorname{span}\{\chi_j | \, j = 1, \ldots, N\}.$$

By χ_j we denote the common nodal basis function from S_h which is 1 at the node X_j and zero at all other nodes.

It is convenient to introduce

$$S_h^l = \left\{\eta^l \in C^0(\Gamma) \,|\, \eta^l(a) = \eta(x(a)), \eta \in S_h \text{ and } x(a) \text{ given by (4.3)}\right\}.$$

In the error analysis of the finite element scheme we shall need the following technical lemmas [10].

Lemma 4.1. *Assume Γ and Γ_h are as above and let d denote the oriented distance function of Γ. Then*

$$\|d\|_{L^\infty(\Gamma_h)} \le ch^2. \tag{4.5}$$

Let δ_h be the quotient between the smooth and discrete surface measures dA on Γ and dA_h on Γ_h so that $\delta_h dA_h = dA$, and let

$$R_h = \frac{1}{\delta_h}\mathcal{P}(\mathcal{I} - d\mathcal{H})\mathcal{P}_h(\mathcal{I} - d\mathcal{H}).$$

Then we have the following estimates

$$\sup_{\Gamma_h} |1 - \delta_h| \le ch^2, \tag{4.6}$$

$$\sup_{\Gamma_h} |(\mathcal{I} - R_h)\mathcal{P}| \le ch^2. \tag{4.7}$$

Lemma 4.2. *Let $\eta : \Gamma_h \to \mathbb{R}$ with lift $\eta^l : \Gamma \to \mathbb{R}$. Then for the planar and curved triangles $e \subset \Gamma_h$ and $T \subset \Gamma$ the following estimates hold. There is a constant $c > 0$ independent of h such that*

$$\frac{1}{c}\|\eta\|_{L^2(e)} \le \|\eta^l\|_{L^2(T)} \le c\|\eta\|_{L^2(e)}, \tag{4.8}$$

$$\frac{1}{c}\|\nabla_{\Gamma_h}\eta\|_{L^2(e)} \le \|\nabla_\Gamma \eta^l\|_{L^2(T)} \le c\|\nabla_{\Gamma_h}\eta\|_{L^2(e)}, \tag{4.9}$$

$$\|\nabla^2_{\Gamma_h}\eta\|_{L^2(e)} \le c\|\nabla^2_\Gamma \eta^l\|_{L^2(T)} + ch\|\nabla_\Gamma \eta^l\|_{L^2(T)}. \tag{4.10}$$

In the above we employ the convention that the L^2 norm of a vector or matrix is simply the L^2 norm of the l^2 norm of the components. We denote by $\nabla^2_\Gamma \eta$ the matrix of second tangential derivatives.

It is convenient to introduce a piecewise linear interpolant which is constructed in an obvious way. Observing that the pointwise linear interpolation $\tilde{I}_h\eta \in S_h$ is well defined for η belonging to $H^2(\Gamma)$, $I_h\eta$ is defined by lifting $\tilde{I}_h\eta$ onto Γ according to (4.2), so that $I_h\eta = (\tilde{I}_h\eta)^l$. The following interpolation results hold, [10].

Lemma 4.3. *For given $\eta \in H^2(\Gamma)$ there exists a unique $I_h\eta \in S_h^l$ such that*

$$\|\eta - I_h\eta\|_{L^2(\Gamma)} + h\|\nabla_\Gamma(\eta - I_h\eta)\|_{L^2(\Gamma)} \le ch^2\left(\|\nabla^2_\Gamma\eta\|_{L^2(\Gamma)} + h\|\nabla_\Gamma\eta\|_{L^2(\Gamma)}\right). \tag{4.11}$$

4.2. Semi-discrete approximation

Our SFEM, based on the finite element spaces introduced in this section, is applicable to all the partial differential equations described in Section 3. Here we give some representative examples. They show that solving partial differential equations on surfaces in $\mathbb{R}^{n+1}$ is analogous to solving equations on domains in $\mathbb{R}^n$. The fourth order problems considered here are treated by the second order splitting approach of [17].

4.2.1. Conservation and diffusion

We begin by describing the semi-discretization of (3.8) in space. Let $(U(\cdot,t),W(\cdot,t)) \in S_h \times S_h$ be such that

$$\int_{\Gamma_h} U_t\phi + \int_{\Gamma_h} \mathcal{D}^{-l}\nabla_{\Gamma_h}W \cdot \nabla_{\Gamma_h}\phi = 0 \quad \forall\phi \in S_h. \tag{4.12}$$

Setting

$$U(\cdot,t) = \sum_{j=1}^{N} \alpha_j(t)\chi_j(\cdot), \quad W(\cdot,t) = \sum_{j=1}^{N} \beta_j(t)\chi_j(\cdot)$$

we find that, $\forall\phi \in S_h$,

$$\int_{\Gamma_h} \sum_{j=1}^{N} \alpha_{j,t}\chi_j\phi + \int_{\Gamma_h} \mathcal{D}^{-l}\sum_{j=1}^{N} \beta_j(t)\nabla_{\Gamma_h}\chi_j \cdot \nabla_{\Gamma_h}\phi = 0$$

and taking $\phi = \chi_k, k = 1,\ldots,N$ we obtain

$$\mathcal{M}\dot{\alpha} + \mathcal{S}\beta = 0 \tag{4.13}$$

where

$$\mathcal{M}_{jk} = \int_{\Gamma_h} \chi_j\chi_k \ , \quad \mathcal{S}_{jk} = \int_{\Gamma_h} \mathcal{D}^{-l}\nabla_{\Gamma_h}\chi_j\nabla_{\Gamma_h}\chi_k.$$

Here $\mathcal{D}^{-l}$ is such that its lift is the diffusivity $\mathcal{D}$ so that $\left(\mathcal{D}^{-l}\right)^l = \mathcal{D}$.

Example 4.4 (Linear diffusion) In this case W=U so that the problem becomes: Find $U(\cdot,t) \in S_h$ such that

$$\int_{\Gamma_h} U_t\phi + \int_{\Gamma_h} \mathcal{D}^{-l}\nabla_{\Gamma_h}U \cdot \nabla_{\Gamma_h}\phi = 0 \quad \forall\phi \in S_h \tag{4.14}$$

yielding the time dependent ordinary differential equations

$$\mathcal{M}\dot{\alpha} + \mathcal{S}\alpha = 0. \tag{4.15}$$

Example 4.5 (Fourth order linear diffusion) In this case we employ the following finite element approximation of (3.18)

$$\int_{\Gamma_h} W\phi - \int_{\Gamma_h} \nabla_{\Gamma_h}U \cdot \nabla_{\Gamma_h}\phi = 0 \quad \forall\phi \in S_h \tag{4.16}$$

which yields $\mathcal{M}\beta - \mathcal{S}^0\alpha = 0$, where

$$\mathcal{S}^0_{jk} = \int_{\Gamma_h} \nabla_{\Gamma_h}\chi_j\nabla_{\Gamma_h}\chi_k.$$

Substituting into (4.13) yields

$$\mathcal{M}\dot{\alpha} + \mathcal{S}\mathcal{M}^{-1}\mathcal{S}^0\alpha = 0. \tag{4.17}$$

Example 4.6 (Surface Cahn Hilliard equation) Find $(U(\cdot,t),W(\cdot,t)) \in S_h \times S_h$ such that

$$\int_{\Gamma_h} U_t\phi + \int_{\Gamma_h} \mathcal{D}^{-l}\nabla_{\Gamma_h}W \cdot \nabla_{\Gamma_h}\phi = 0 \quad \forall\phi \in S_h, \tag{4.18}$$

$$\int_{\Gamma_h} \epsilon\nabla_{\Gamma_h}U \cdot \nabla_{\Gamma_h}\phi + \frac{\tilde{I}_h\Psi'(U)}{\epsilon}\phi = \int_{\Gamma_h} W\phi \quad \forall\phi \in S_h. \tag{4.19}$$

Note the use of $\tilde{I}_h\Psi'(U)$. The discrete equations become

$$\mathcal{M}\dot{\alpha} + \mathcal{S}\beta = 0, \quad \mathcal{M}\beta - \epsilon\mathcal{S}^0\alpha - \frac{1}{\epsilon}\mathcal{M}\Psi'(\alpha) = 0$$

and eliminating β we obtain

$$\mathcal{M}\dot{\alpha} + \epsilon\mathcal{S}\mathcal{M}^{-1}\mathcal{S}^0\alpha + \frac{1}{\epsilon}\mathcal{S}\Psi'(\alpha) = 0. \tag{4.20}$$

Here we use the notation that $(\Psi'(\alpha))_j = \Psi'(\alpha_j)$.

4.2.2. Equations in non-conservation form

Example 4.7 (Surface Allen-Cahn equation) The approximate problem is to find $U(\cdot,t) \in S_h$ such that

$$\epsilon\int_{\Gamma_h} U_t\phi + \int_{\Gamma_h}\left(\epsilon\nabla_{\Gamma_h}U\cdot\nabla_{\Gamma_h}\phi + \frac{1}{\epsilon}\tilde{I}_h\Psi'(U)\phi\right) = 0 \quad \forall\phi\in S_h, \tag{4.21}$$

which may be rewritten in matrix form as

$$\epsilon\mathcal{M}\dot{\alpha} + \epsilon\mathcal{S}^0\alpha + \frac{1}{\epsilon}\mathcal{M}\Psi'(\alpha) = 0. \tag{4.22}$$

Example 4.8 (Level set geodesic mean curvature flow) The semi-discrete finite element approximation is: Find $U(\cdot,t)\in S_h$ such that

$$\int_{\Gamma_h}\frac{U_t}{|\nabla_{\Gamma_h}U|_\epsilon}\phi + \int_{\Gamma_h}\frac{\nabla_{\Gamma_h}U}{|\nabla_{\Gamma_h}U|_\epsilon}\cdot\nabla_{\Gamma_h}\phi = 0 \quad \forall\phi\in S_h. \tag{4.23}$$

Here we have introduced the following regularized l^2 norm $|p|_\epsilon = \sqrt{|p|^2+\epsilon^2}$ in order to avoid dividing by zero when $\nabla_{\Gamma_h}U = 0$. It follows that the discrete equations may be written as

$$\mathcal{M}_U\dot{\alpha} + \mathcal{S}_U\alpha = 0 \tag{4.24}$$

where the weighted mass and stiffness matrices are

$$(M_U)_{jk} = \int_{\Gamma_h}\frac{\chi_j\chi_k}{|\nabla_{\Gamma_h}U|_\epsilon}\ , \quad (S_U)_{jk} = \int_{\Gamma_h}\frac{\nabla_{\Gamma_h}\chi_j\nabla_{\Gamma_h}\chi_k}{|\nabla_{\Gamma_h}U|_\epsilon}.$$

Example 4.9 (Level set geodesic surface diffusion) Find $(U(\cdot,t),W(\cdot,t))\in S_h\times S_h$ such that

$$\int_{\Gamma_h} U_t\phi + \int_{\Gamma_h}|\nabla_{\Gamma_h}U|\mathcal{P}_g^h\nabla_{\Gamma_h}W\cdot\nabla_{\Gamma_h}\phi = 0 \quad \forall\phi\in S_h, \tag{4.25}$$

$$\int_{\Gamma_h} W\phi + \int_{\Gamma_h}\frac{\nabla_{\Gamma_h}U}{|\nabla_\Gamma U|_\epsilon}\cdot\nabla_{\Gamma_h}\phi = 0 \quad \forall\phi\in S_h. \tag{4.26}$$

Here we have used the notation

$$\nu_g^h = \frac{\nabla_{\Gamma_h}U}{|\nabla_{\Gamma_h}U|_\epsilon}, \quad \mathcal{P}_g^h = \mathcal{I} - \nu_g^h\otimes\nu_g^h.$$

The discrete equations become

$$\mathcal{M}\dot{\alpha} + \mathcal{S}_g^h\beta = 0, \quad \mathcal{M}\beta - \mathcal{S}_U\alpha = 0,$$

and eliminating β we obtain

$$\mathcal{M}\dot{\alpha} + \mathcal{S}_g^h\mathcal{M}^{-1}\mathcal{S}_U\alpha = 0, \tag{4.27}$$

where

$$(\mathcal{S}_g^h)_{jk} = \int_{\Gamma_h}|\nabla_{\Gamma_h}U|\mathcal{P}_g^h\nabla_{\Gamma_h}\chi_j\nabla_{\Gamma_h}\chi_k.$$

5. Error Bounds

In this section we will prove convergence results for the parabolic plate equation on a surface Γ. We do this in order to give a nontrivial example for our approximation methods. Several of the equations discussed in the previous sections can be treated along the lines of the convergence proof for the parabolic plate equation on a surface. In order to simplify the presentation we treat the case $\mathcal{D} = \mathcal{I}$ only.

5.1. Linear Diffusion

Lemma 5.1 (Stability) *Let U, W be a solution of the semi-discrete scheme as in Example 3.8 with initial value $U(\cdot,0) = U_0$ and U^l, W^l its lift according to* (4.2). *Then the following stability estimates hold:*

$$\sup_{(0,T)} \|U^l\|^2_{L^2(\Gamma)} + \int_0^T \|W^l\|^2_{L^2(\Gamma)} \le c\|U^l_0\|^2_{L^2(\Gamma)}, \tag{5.1}$$

$$\int_0^T \|U^l_t\|^2_{L^2(\Gamma)} + \sup_{(0,T)} \|W^l\|^2_{L^2(\Gamma)} \le c\|W^l(\cdot,0)\|^2_{L^2(\Gamma)}, \tag{5.2}$$

$$\sup_{(0,T)} \|\nabla_\Gamma U^l\|^2_{L^2(\Gamma)} + \int_0^T \|\nabla_\Gamma W^l\|^2_{L^2(\Gamma)} \le c(\|U^l_0\|^2_{L^2(\Gamma)} + \|W^l(\cdot,0)\|^2_{L^2(\Gamma)}). \tag{5.3}$$

Proof. If we test the diffusion equation (4.12) with $\phi = U_t$ and take the time derivative of the equation (4.16) and then test that equation with $\phi = W$ and take the sum of the two resulting equations we get

$$\int_{\Gamma_h} U_t^2 + \frac{1}{2}\frac{d}{dt}\int_{\Gamma_h} W^2 = 0,$$

which leads to the estimate (5.2).

Choosing $\phi = U$ in (4.12), $\phi = W$ in (4.16) and taking the sum leads to

$$\frac{1}{2}\frac{d}{dt}\int_{\Gamma_h} U^2 + \int_{\Gamma_h} W^2 = 0$$

and this gives the estimate (5.1).

The estimate (5.3) follows by taking $\phi = U$ in (4.16) with the use of the previous estimates. Similarly the choice $\phi = W$ in (4.12) gives the estimate for the gradient of W.

We now can prove a convergence result for piecewise linear finite elements on two dimensional surfaces. Note that as discrete initial value we take a realistic function which can be computed.

Theorem 5.2 (Convergence) *Let $u, w = -\Delta_\Gamma u$ be a sufficiently smooth solution of*

$$u_t + \Delta_\Gamma^2 u = 0, \quad u(\cdot,0) = u_0 \quad on \quad \Gamma$$

on the sufficiently smooth closed surface Γ and let U, W be the discrete solution according to (4.12) *and* (4.16). *As initial value U_0 we take the discrete Ritz projection of the continuous initial value u_0 defined by*

$$\int_{\Gamma_h} \nabla_{\Gamma_h} U_0 \cdot \nabla_{\Gamma_h}\phi = \int_{\Gamma_h} \nabla_{\Gamma_h} u_0^{-l} \cdot \nabla_{\Gamma_h}\phi \quad \forall \phi \in S_h \tag{5.4}$$

and $\int_{\Gamma_h} U_0 = 0$. *With the lifts* U^l *of* U *and* W^l *of* W *we then have the error estimates*

$$\sup_{t\in(0,T)} \|u(\cdot,t) - U^l(\cdot,t)\|_{L^2(\Gamma)} + h \sup_{t\in(0,T)} \|\nabla_\Gamma(u(\cdot,t) - U^l(\cdot,t))\|_{L^2(\Gamma)} \le C_1 h^2, \tag{5.5}$$

and

$$\left(\int_0^T \|w(\cdot,t) - W^l(\cdot,t)\|^2_{L^2(\Gamma)}\,dt\right)^{\frac{1}{2}} + h\left(\int_0^T \|\nabla_\Gamma(w(\cdot,t) - W^l(\cdot,t))\|^2_{L^2(\Gamma)}\,dt\right)^{\frac{1}{2}} \le C_2 h^2, \tag{5.6}$$

where

$$C_1 = c(\sup_{t\in(0,T)} \|u(\cdot,t)\|_{H^4(\Gamma)} + \left(\int_0^T \|u_t(\cdot,t)\|^2_{H^2(\Gamma)}dt\right)^{\frac{1}{2}} + \|u_0\|_{H^4(\Gamma)}),$$
$$C_2 = c(\left(\int_0^T \|u(\cdot,t)\|^2_{H^4(\Gamma)}\right)^{\frac{1}{2}} + \left(\int_0^T \|u_t(\cdot,t)\|^2_{H^2(\Gamma)}\,dt\right)^{\frac{1}{2}} + \|u_0\|_{H^4(\Gamma)}).$$

Proof. In order to make the proof clearer we only treat the case $\mathcal{D} = \mathcal{I}$ here. The proof is easily extended to the general case. The error bounds follow the classic Galerkin error analysis for parabolic equations [28] and rely on a suitable form of the error equation. In order to compare discrete and continuous solution both should be defined on the same surface which we take to be the continuous surface Γ. The continuous equations read

$$\int_\Gamma u_t\varphi + \int_\Gamma \nabla_\Gamma w \cdot \nabla_\Gamma \varphi = 0, \quad \int_\Gamma w\psi - \int_\Gamma \nabla_\Gamma u \cdot \nabla_\Gamma \psi = 0 \tag{5.7}$$

for all $\varphi, \psi \in H^1(\Gamma)$, and the discrete equations are given by

$$\int_{\Gamma_h} U_t\phi + \int_{\Gamma_h} \nabla_{\Gamma_h} W \cdot \nabla_{\Gamma_h}\phi = 0, \quad \int_{\Gamma_h} W\psi - \int_{\Gamma_h} \nabla_{\Gamma_h} U \cdot \nabla_{\Gamma_h}\psi = 0 \tag{5.8}$$

for all $\phi, \psi \in S_h$. We lift the discrete equations to the continuous surface as it was described in (4.2). We define U^l, W^l and ϕ^l, ψ^l by

$$U(x,t) = U^l(a(x),t), \quad W(x,t) = W^l(a(x),t),$$
$$\phi(x) = \phi^l(a(x)), \quad \psi(x) = \psi^l(a(x))$$

for points $x \in \Gamma_h$. For better understanding of the following, we introduce the notation

$$u_h(x,t) = U^l(x,t), \quad w_h(x,t) = W^l(x,t), \quad x \in \Gamma.$$

We recall the abbreviation (see Lemma 4.1)

$$R_h(x) = \frac{1}{\delta_h(x)}\mathcal{P}(x)(I - d(x)\mathcal{H}(x))\mathcal{P}_h(x)(I - d(x)\mathcal{H}(x)), \quad x \in \Gamma_h$$

together with its lifted version $R_h^l(a(x)) = R_h(x)$, $x \in \Gamma_h$. Thus (5.8) leads to

$$\int_\Gamma u_{h,t}\varphi_h \frac{1}{\delta_h^l} + \int_\Gamma R_h^l \nabla_\Gamma w_h \cdot \nabla_\Gamma \varphi_h = 0, \int_\Gamma w_h\psi_h \frac{1}{\delta_h^l} - \int_\Gamma R_h^l \nabla_\Gamma u_h \cdot \nabla_\Gamma \psi_h = 0 \tag{5.9}$$

for all $\varphi_h, \psi_h \in S_h^l$. We take the differences of the equations (5.7) at φ_h, ψ_h and (5.9).

The error relation between continuous and lifted discrete solution then is given by

$$\int_\Gamma (u_t - \frac{1}{\delta_h^l} u_{h,t})\varphi_h + \int_\Gamma \left(\nabla_\Gamma w - R_h^l \nabla_\Gamma w_h\right) \cdot \nabla_\Gamma \varphi_h = 0, \tag{5.10a}$$

$$\int_\Gamma (w - \frac{1}{\delta_h^l} w_h)\psi_h - \int_\Gamma \left(\nabla_\Gamma u - R_h^l \nabla_\Gamma u_h\right) \cdot \nabla_\Gamma \psi_h = 0 \tag{5.10b}$$

for all $\varphi_h, \psi_h \in S_h^l$, and with the use of the estimates from Lemma 4.1 we obtain

$$\int_\Gamma (u - u_h)_t \varphi_h + \int_\Gamma \nabla_\Gamma (w - w_h) \cdot \nabla_\Gamma \varphi_h \le ch^2 \int_\Gamma (|\nabla_\Gamma w_h||\nabla_\Gamma \varphi_h| + |u_{h,t}||\varphi_h|), \tag{5.11a}$$

$$\int_\Gamma (w - w_h)\psi_h - \int_\Gamma \nabla_\Gamma (u - u_h) \cdot \nabla_\Gamma \psi_h \le ch^2 \int_\Gamma (|\nabla_\Gamma u_h||\nabla_\Gamma \psi_h| + |w_h||\psi_h|) \tag{5.11b}$$

for all $\varphi_h, \psi_h \in S_h^l$.

We define the Ritz-Galerkin projection $\tilde{v}_h$ of a function v as the unique solution $\tilde{v}_h \in S_h^l$ with $\int_\Gamma \tilde{v}_h = 0$ of

$$\int_\Gamma \nabla_\Gamma \tilde{v}_h \cdot \nabla_\Gamma \varphi_h = \int_\Gamma \nabla_\Gamma v \cdot \nabla_\Gamma \varphi_h \quad \forall \varphi_h \in S_h^l. \tag{5.12}$$

It is easily shown, with the help of Lemma 4.3, that for a sufficiently smooth function v one has the estimates

$$\|v - \tilde{v}_h\|_{L^2(\Gamma)} + h\|\nabla_\Gamma (v - \tilde{v}_h)\|_{L^2(\Gamma)} \le ch^2 \|v\|_{H^2(\Gamma)} \tag{5.13}$$

and similar estimates for the time derivative of v if $v_t \in H^2(\Gamma)$.

We now use $\varphi_h = \tilde{u}_h - u_h$ and $\psi_h = \tilde{w}_h - w_h$ as test functions in (5.11), take the sum of the two resulting equations, and arrive at

$$\begin{aligned}
&\frac{1}{2}\frac{d}{dt}\|\tilde{u}_h - u_h\|_{L^2(\Gamma)}^2 + \|\tilde{w}_h - w_h\|_{L^2(\Gamma)}^2 \\
&\le \|\tilde{u}_{h,t} - u_t\|_{L^2(\Gamma)}\|\tilde{u}_h - u_h\|_{L^2(\Gamma)} + \|\tilde{w}_h - w\|_{L^2(\Gamma)}\|\tilde{w}_h - w_h\|_{L^2(\Gamma)} \\
&\quad + ch^2\left(\|\nabla_\Gamma w_h\|_{L^2(\Gamma)}\|\nabla_\Gamma(\tilde{u}_h - u_h)\|_{L^2(\Gamma)} + \|u_{h,t}\|_{L^2(\Gamma)}\|\tilde{u}_h - u_h\|_{L^2(\Gamma)}\right) \\
&\quad + ch^2\left(\|\nabla_\Gamma u_h\|_{L^2(\Gamma)}\|\nabla_\Gamma(\tilde{w}_h - w_h)\|_{L^2(\Gamma)} + \|w_h\|_{L^2(\Gamma)}\|\tilde{w}_h - w_h\|_{L^2(\Gamma)}\right) \\
&\le \varepsilon\|\tilde{u}_h - u_h\|_{L^2(\Gamma)}^2 + \frac{1}{2}\|\tilde{w}_h - w_h\|_{L^2(\Gamma)}^2 \\
&\quad + c_\varepsilon h^4\Big(\|\nabla_\Gamma u_h\|_{L^2(\Gamma)}^2 + \|\nabla_\Gamma w_h\|_{L^2(\Gamma)}^2 + \|u_{h,t}\|_{L^2(\Gamma)}^2 + \|w_h\|_{L^2(\Gamma)}^2 + \|u_t\|_{H^2(\Gamma)}^2 \\
&\quad + \|w\|_{H^2(\Gamma)}^2\Big) + \varepsilon\|\nabla_\Gamma(\tilde{u}_h - u_h)\|_{L^2(\Gamma)}^2 + \varepsilon\|\nabla_\Gamma(\tilde{w}_h - w_h)\|_{L^2(\Gamma)}^2.
\end{aligned} \tag{5.14}$$

Here ε is a positive number which will be chosen later. The last two terms on the right hand side of this inequality are treated as follows. In (5.10) we choose $\varphi_h = \tilde{w}_h - w_h$ and $\psi_h = \tilde{u}_{h,t} - u_{h,t}$ as test functions and subtract the resulting equations. Thus

$$\begin{aligned}
&\int_\Gamma (\nabla_\Gamma \tilde{w}_h - R_h^l \nabla_\Gamma w_h) \cdot \nabla_\Gamma(\tilde{w}_h - w_h) + \int_\Gamma (\nabla_\Gamma \tilde{u}_h - R_h^l \nabla_\Gamma u_h) \cdot \nabla_\Gamma(\tilde{u}_{h,t} - u_{h,t}) \\
&= -\int_\Gamma \left((u_t - \frac{1}{\delta_h^l} u_{h,t})(\tilde{w}_h - w_h) - (w - \frac{1}{\delta_h^l} w_h)(\tilde{u}_{h,t} - u_{h,t})\right).
\end{aligned} \tag{5.15}$$

We estimate the terms in this equation separately. For the first term on the left hand side we have with Lemma 4.1

$$
\begin{aligned}
&\int_\Gamma (\nabla_\Gamma \tilde{w}_h - R_h^l \nabla_\Gamma w_h) \cdot \nabla_\Gamma (\tilde{w}_h - w_h) \\
&\geq \int_\Gamma |\nabla_\Gamma (\tilde{w}_h - w_h)|^2 - ch^2 \int_\Gamma |\nabla_\Gamma w_h| |\nabla_\Gamma (\tilde{w}_h - w_h)| \\
&\geq \frac{1}{2} \int_\Gamma |\nabla_\Gamma (\tilde{w}_h - w_h)|^2 - ch^4 \int_\Gamma |\nabla_\Gamma w_h|^2.
\end{aligned} \tag{5.16}
$$

The second term on the left hand side of (5.15) is treated as follows:

$$
\begin{aligned}
&\int_\Gamma (\nabla_\Gamma \tilde{u}_h - R_h^l \nabla_\Gamma u_h) \cdot \nabla_\Gamma (\tilde{u}_{h,t} - u_{h,t}) \\
&\geq \frac{1}{2} \frac{d}{dt} \int_\Gamma R_h^l \nabla_\Gamma (\tilde{u}_h - u_h) \cdot \nabla_\Gamma (\tilde{u}_h - u_h) + \frac{d}{dt} \int_\Gamma (I - R_h^l) \nabla_\Gamma \tilde{u}_h \cdot \nabla_\Gamma (\tilde{u}_h - u_h) \\
&\quad - \varepsilon \int_\Gamma |\nabla_\Gamma (\tilde{u}_h - u_h)|^2 - c_\varepsilon h^4 \int_\Gamma |\nabla_\Gamma \tilde{u}_{h,t}|^2.
\end{aligned} \tag{5.17}
$$

Here we have used the symmetry of the matrix $\mathcal{P} R_h^l \mathcal{P}$.

And the right hand side of (5.15) is rewritten as

$$
\begin{aligned}
&\int_\Gamma \Big((u_t - \frac{1}{\delta_h^l} u_{h,t})(\tilde{w}_h - w_h) - (w - \frac{1}{\delta_h^l} w_h)(\tilde{u}_{h,t} - u_{h,t}) \Big) \\
&= \frac{d}{dt} \int_\Gamma (u - u_h)(\frac{1}{\delta_h^l} \tilde{w}_h - w) - \int_\Gamma (u - u_h)(\frac{1}{\delta_h^l} \tilde{w}_{h,t} - w_t) \\
&\quad + \int_\Gamma (u_t - \tilde{u}_{h,t})(w - w_h) + \int_\Gamma (u_t \tilde{w}_h - \tilde{u}_{h,t} w_h)(1 - \frac{1}{\delta_h^l}) \\
&\geq \frac{d}{dt} \int_\Gamma (u - u_h)(\frac{1}{\delta_h^l} \tilde{w}_h - w) - \varepsilon \int_\Gamma (\tilde{u}_h - u_h)^2 - \varepsilon \int_\Gamma (\tilde{w}_h - w_h)^2 \\
&\quad - c_\varepsilon h^4 (\|u\|_{H^2(\Gamma)}^2 + \|u_t\|_{H^2(\Gamma)}^2 + \|w\|_{H^2(\Gamma)}^2 + \|w_t\|_{H^2(\Gamma)}^2).
\end{aligned} \tag{5.18}
$$

We now collect the estimates (5.16), (5.17) and (5.18), integrate with respect to time. For $h \leq h_0$ this gives the estimate

$$
\begin{aligned}
&\|\nabla_\Gamma (\tilde{u}_h - u_h)\|_{L^2(\Gamma)}^2 + \int_0^t \|\nabla_\Gamma (\tilde{w}_h - w_h)\|_{L^2(\Gamma)}^2 \, dt \\
&\leq \varepsilon \|\tilde{u}_h - u_h\|_{L^2(\Gamma)}^2 + \varepsilon \int_0^t \|\tilde{u}_h - u_h\|_{H^1(\Gamma)}^2 \, dt + \varepsilon \int_0^t \|\tilde{w}_h - w_h\|_{L^2(\Gamma)}^2 \, dt \\
&\quad + c_\varepsilon h^4 \left(\|u\|_{H^2(\Gamma)}^2 + \|w\|_{H^2(\Gamma)}^2 + \int_0^t \|u\|_{H^2(\Gamma)}^2 + \|w\|_{H^2(\Gamma)}^2 \, dt \right) + A_{0,h}.
\end{aligned} \tag{5.19}
$$

By $A_{0,h}$ we denote the contribution of the initial values

$$
\begin{aligned}
A_{0.h} = &\frac{1}{2} \int_\Gamma R_h^l \nabla_\Gamma (\tilde{u}_h(\cdot,0) - u_h(\cdot,0)) \cdot \nabla_\Gamma (\tilde{u}_h(\cdot,0) - u_h(\cdot,0)) \\
&+ \int_\Gamma (I - R_h^l) \nabla_\Gamma \tilde{u}_h(\cdot,0) \cdot \nabla_\Gamma (\tilde{u}_h(\cdot,0) - u_h(\cdot,0)) \\
&+ \int_\Gamma (u_0 - u_h(\cdot,0))(\frac{1}{\delta_h^l} \tilde{w}_h(\cdot,0) - w(\cdot,0)).
\end{aligned}
$$

Our choice of $u_{h0} = U_0^l$ (see (5.4)) leads to

$$\|\nabla_\Gamma(\tilde{u}_h(\cdot,0) - u_{h0})\|_{L^2(\Gamma)} \le ch^3 \|u_0\|_{H^2(\Gamma)}, \tag{5.20}$$

$$\|\tilde{u}_h(\cdot,0) - u_{h0}\|_{L^2(\Gamma)} \le ch^2 \|u_0\|_{H^2(\Gamma)}. \tag{5.21}$$

This estimate is left to the reader. It is an easy consequence of the definition of the discrete initial value, the geometric estimates from Lemma 4.1 and the assumptions on the mean values of $\tilde{u}_h(\cdot,0)$ and u_{h0}.

Altogether we arrive at the following estimate for the gradient terms:

$$\begin{aligned}
&\|\nabla_\Gamma(\tilde{u}_h - u_h)\|^2_{L^2(\Gamma)} + \int_0^t \|\nabla_\Gamma(\tilde{w}_h - w_h)\|^2_{L^2(\Gamma)}\,dt \\
&\le \varepsilon\|\tilde{u}_h - u_h\|^2_{L^2(\Gamma)} + \varepsilon\int_0^t \|\tilde{u}_h - u_h\|^2_{H^1(\Gamma)}\,dt + \varepsilon\int_0^t \|\tilde{w}_h - w_h\|^2_{L^2(\Gamma)}\,dt \\
&\quad + c_\varepsilon h^4\left(\|u\|^2_{H^2(\Gamma)} + \|w\|^2_{H^2(\Gamma)} + \int_0^t \|u\|^2_{H^2(\Gamma)} + \|w\|^2_{H^2(\Gamma)}\,dt + \|u_0\|^2_{H^2(\Gamma)}\right).
\end{aligned} \tag{5.22}$$

We now integrate estimate (5.14) with respect to time and get

$$\begin{aligned}
&\|\tilde{u}_h - u_h\|^2_{L^2(\Gamma)} + \int_0^t \|\tilde{w}_h - w_h\|^2_{L^2(\Gamma)}\,dt \\
&\le \varepsilon\int_0^t \|\tilde{u}_h - u_h\|^2_{H^1(\Gamma)}\,dt + \varepsilon\int_0^t \|\nabla_\Gamma(\tilde{w}_h - w_h)\|^2_{L^2(\Gamma)}\,dt + c_\varepsilon h^4\left(\int_0^t \|\nabla_\Gamma u_h\|^2_{L^2(\Gamma)}\right. \\
&\quad \left. + \|w_h\|^2_{H^1(\Gamma)} + \|u_{h,t}\|^2_{L^2(\Gamma)} + \|u_t\|^2_{H^2(\Gamma)} + \|w\|^2_{H^2(\Gamma)}\,dt\right) + ch^4\|u_0\|^2_{H^2(\Gamma)}.
\end{aligned} \tag{5.23}$$

We now add the estimates (5.22) and (5.23) and choose ε small enough to obtain

$$\begin{aligned}
&\|\tilde{u}_h - u_h\|^2_{H^1(\Gamma)} + \int_0^t \|\tilde{w}_h - w_h\|^2_{H^1(\Gamma)}\,dt \\
&\le \int_0^t \|\tilde{u}_h - u_h\|^2_{H^1(\Gamma)}\,dt \quad + ch^4\int_0^t \|\nabla_\Gamma u_h\|^2_{L^2(\Gamma)} + \|w_h\|^2_{H^1(\Gamma)} + \|u_{h,t}\|^2_{L^2(\Gamma)}\,dt \\
&\quad + ch^4\int_0^t \|u_t\|^2_{H^2(\Gamma)} + \|u\|^2_{H^2(\Gamma)} + \|w\|^2_{H^2(\Gamma)}\,dt \\
&\quad + ch^4\left(\|u\|^2_{H^2(\Gamma)} + \|w\|^2_{H^2(\Gamma)} + \|u_0\|^2_{H^2(\Gamma)} + \|w(\cdot,0)\|^2_{H^2(\Gamma)}\right).
\end{aligned} \tag{5.24}$$

After an additional Gronwall argument we deduce the final estimate

$$\begin{aligned}
&\sup_{(0,T)}\|\tilde{u}_h - u_h\|^2_{H^1(\Gamma)} + \int_0^T \|\tilde{w}_h - w_h\|^2_{H^1(\Gamma)}\,dt \\
&\le ch^4\Big(\int_0^T \|u_{h,t}\|^2_{L^2(\Gamma)} + \|\nabla_\Gamma u_h\|^2_{L^2(\Gamma)} + \|w_h\|^2_{H^1(\Gamma)}\,dt \\
&\quad + \|u_0\|^2_{H^4(\Gamma)} + \int_0^T \|u_t\|^2_{H^2(\Gamma)} + \|u\|^2_{H^4(\Gamma)}\,dt\Big).
\end{aligned}$$

The stability estimates from Lemma 5.1 together with the error estimates for the Ritz-Galerkin projections finally prove the theorem.

We finally mention how the initial value of W is treated. For the estimate of $\|W^l(\cdot,0)\|_{L^2(\Gamma)}$ we use an inverse inequality. From (4.16) and (5.4) we infer

$$\begin{aligned}
\|W(\cdot,0)\|^2_{L^2(\Gamma_h)} &= \int_{\Gamma_h} \nabla_{\Gamma_h} U_0 \cdot \nabla_{\Gamma_h} W(\cdot,0) = \int_{\Gamma_h} \nabla_{\Gamma_h} u_0^{-l} \cdot \nabla_{\Gamma_h} W(\cdot,0) \\
&= \int_\Gamma R_h^l \nabla_\Gamma u_0 \cdot \nabla_\Gamma W^l(\cdot,0) = \int_\Gamma (R_h^l - \mathcal{I}) \nabla_\Gamma u_0 \cdot \nabla_\Gamma W^l(\cdot,0) + \int_\Gamma \nabla_\Gamma u_0 \cdot \nabla_\Gamma W^l(\cdot,0) \\
&\leq ch^2 \|\nabla_\Gamma u_0\|_{L^2(\Gamma)} \|\nabla_\Gamma W^l(\cdot,0)\|_{L^2(\Gamma)} + \|\Delta_\Gamma u_0\|_{L^2(\Gamma)} \|W^l(\cdot,0)\|_{L^2(\Gamma)} \\
&\leq ch^2 \|\nabla_\Gamma u_0\|_{L^2(\Gamma)} \|\nabla_{\Gamma_h} W(\cdot,0)\|_{L^2(\Gamma_h)} + c\|u_0\|_{H^2(\Gamma)} \|W(\cdot,0)\|_{L^2(\Gamma)} \\
&\leq c\|u_0\|_{H^2(\Gamma)} \|W(\cdot,0)\|_{L^2(\Gamma_h)},
\end{aligned}$$

and so,

$$\|W(\cdot,0)\|_{L^2(\Gamma_h)} \leq c\|u_0\|_{H^2(\Gamma)}.$$

6. Implementation

For our computations we used the same time discretizations as in the Cartesian case. For the linear problems these were the standard first order implicit time discretizations. For the nonlinear problems time discretizations were used to linearize the problem. A survey of such time discretizations can be found in [6, 16, 18]. The resulting linear systems were solved with CG algorithms.

Algorithm 6.1 (Element stiffness matrix)

For a given triangle e with vertices $a_0, a_1, a_2 \in \mathbb{R}^3$ calculate the area

$$\text{area} = \frac{1}{2} |(a_1 - a_0) \wedge (a_2 - a_0)|,$$

calculate the vectors

$$\begin{aligned}
b_k &= a_{k+1} - a_k \quad (k = 0,1,2 \bmod 3), \\
c_k &= b_k \cdot b_{k+1}\, b_{k-1} - b_k \cdot b_{k-1}\, b_{k+1} \quad (k = 0,1,2 \bmod 3),
\end{aligned}$$

and then set up the element stiffness matrix as

$$\mathcal{S}^e_{ij} = \frac{1}{16 \text{ area}}\, c_i \cdot c_j \quad (i,j = 0,1,2).$$

We would like to point out that the implementations of the fully discrete schemes are nearly the same as for plane problems. The only difference for the finite element code is that the nodes lie in $\mathbb{R}^{n+1}$. A finite element program sets up the stiffness matrix, the mass matrix and the right hand side of the linear system by looping over all triangles. In this loop it visits each element once and computes the element stiffness matrix, the element mass matrix and the element right hand side and sums the result to the correct places in the matrices or the right hand side. In order to demonstrate the simplicity of the algorithm we give a program, Algorithm 6.1, for the computation of the element stiffness matrix

$$\mathcal{S}^e_{ij} = \int_e \nabla_\Gamma \chi^e_i \cdot \nabla_\Gamma \chi^e_j = \int_e \nabla_e \chi^e_i \cdot \nabla_e \chi^e_j, \qquad i,j = 0,1,2$$

for two dimensional surfaces in three space dimensions. Here $\chi_0^e, \chi_1^e, \chi_2^e$ are the element basis functions, i.e., the restrictions of the global basis functions to the element e. Note that in the definition of the element stiffness matrix the tangential gradients become Cartesian gradients because e is planar. In the formula for the area "$\wedge$" denotes the vector product in $\mathbb{R}^3$.

7. Concluding Remarks

The approach described here is directly applicable to other boundary conditions when $\partial\Gamma$ is non-empty such as the non-homogeneous Dirichlet condition

$$u = g \quad \text{on} \quad \partial\Gamma,$$

or Neumann boundary condition

$$\nabla_\Gamma u \cdot \mu = g \quad \text{on} \quad \partial\Gamma.$$

The method could be developed to apply to a coupling with field equations away from the surface.

Observe that the approximating surfaces are polyhedral. It is a challenge to extend this approach to higher order approximations of the surface and higher order finite element methods. Although the exposition has been concerned with triangulated surfaces in $\mathbb{R}^3$, immediately applicable to curves, the methodology is also applicable to hypersurfaces in higher space dimensions. Furthermore equations can be solved by this approach on surfaces with self-intersections and on non-oriented surfaces.

Acknowledgements. This work was began whilst the authors participated in the 2003 programme *Computational Challenges in Partial Differential Equations* at the Isaac Newton Institute, Cambridge, UK. The graphical presentations were performed with the package GRAPE.

References

[1] D. Adalsteinsson and J.A. Sethian, Transport and diffusion of material quantities on propagating interfaces via level set methods, *J. Comput. Phys.*, **185** (2003), 271-288.

[2] Th. Aubin, Nonlinear Analysis on Manifolds. Monge-Ampère Equations, Springer, Berlin-Heidelberg-New York, 1982.

[3] M. Bertalmio, L.T. Cheng, S. Osher and G. Sapiro, Variational problems and partial differential equations on implicit surfaces, *J. Comput. Phys.*, **174** (2001), 759-780.

[4] M. Burger, Finite element approximation of elliptic partial differential equations on implicit surfaces, *Comput. Visual. Sci.*, (2007), to appear.

[5] U. Clarenz, U. Diewald, G. Dziuk, M. Rumpf and R. Rusu, A finite element method for surface restoration with smooth boundary conditions, *Comput. Aid. Geom. Des.*, **21** (2004), 427-445.

[6] K. Deckelnick, G. Dziuk and C.M. Elliott, Computation of geometric PDEs and mean curvature flow, *Acta Numerica*, (2005), 139-232.

[7] K. Deckelnick, C.M. Elliott and V. Styles, Numerical diffusion induced grain boundary motion, *Interface. Free Bound.*, **3** (2001), 393-414.

[8] J. Dogel, R. Tsekov and W. Freyland, Two dimensional connective nano-structures of electrodeposited Zn on Au (111) induced by spinodal decomposition, *J. Chem. Phys.*, **122** (2005), 1-8.

[9] Q. Du and L. Ju, Approximations of a Ginzburg-Landau model for superconducting hollow spheres based on spherical centroidal Voroni tesselations, *Math. Comput.*, **74** (2005), 1257-1280.

[10] G. Dziuk, Finite Elements for the Beltrami operator on arbitrary surfaces, In: S. Hildebrandt, R. Leis (Herausgeber): Partial Differential Equations and Calculus of Variations. Lecture Notes in Mathematics, Springer, **1357** (1988), 142-155.

[11] G. Dziuk, An algorithm for evolutionary surfaces, *Numer. Math.*, **58** (1991), 603-611.

[12] G. Dziuk and C.M. Elliott, Finite elements on evolving surfaces, *IMA J. Numer. Anal.*, **27** (2007), 262-292.

[13] G. Dziuk and C.M. Elliott, Eulerian finite element method for parabolic PDES on implicit surfaces, *Interface. Free Bound.*, (2006), submitted.

[14] G. Dziuk and C.M. Elliott, Eulerian level set method for PDEs on evolving surfaces, (2006), in preparation.

[15] K. Ecker, Regularity theory for mean curvature flow, Progress in Nonlinear Differential Equations and Their Applications, **57**, Birkhauser, (2004).

[16] C.M. Elliott, The Cahn-Hilliard model for the kinetics of phase separation. In Mathematical Models for Phase Change Problems, J.F. Rodrigues (Ed.), International Series of Numerical Mathematics **88**, Birkhauser Verlag, (1989), 35-73.

[17] C.M. Elliott, D. French and F. Milner, A second order splitting method for the Cahn-Hilliard equation, *Numer. Math.*, **54** (1989), 575-590.

[18] C.M. Elliott and A. Stuart, The global dynamics of discrete semilinear parabolic equations, *SIAM J. Numer. Anal.*, **30** (1993), 1622-1663.

[19] P. Fife, J.W. Cahn and C.M. Elliott, A free boundary model for diffusion induced grain boundary motion, *Interface. Free Bound.*, **3** (2001), 291-336.

[20] D. Gilbarg and N.S. Trudinger, Elliptic Partial Differential Equations of Second Order, Springer, 1988.

[21] J. Greer, A. Bertozzi and G. Sapiro, Fourth order partial differential equations on general geometries, *J. Comput. Phys.*, **216**:1 (2006), 216-246.

[22] R. Kimmel, Intrinsic scale space for images on surfaces: The geodesic curvature flow, *Graph. Models Image Process.*, **59** (1997), 365-372.

[23] U.F. Mayer and G. Simonett, Classical solutions for diffusion induced grain boundary motion, *J. Math. Anal.*, **234** (1999), 660-674.

[24] F. Memoli, G. Sapiro and P. Thompson, Implicit brain imaging, *NeuroImage*, **23** (2004), S179-S188.

[25] A. Ratz and A. Voigt, PDEs on surfaces–a diffuse interface approach, *Commun. Math. Sci.*, **4** (2006), 575-590.

[26] O. Schönborn, R. C. Desai, Kinetics of phase ordering on curved surfaces, *Physica A*, **239** (1997), 412-419.

[27] P. Tang, F. Qiu, H. Zhang and Y. Yang, Phase separation patterns for diblock copolymers on spherical surfaces: A finite volume method, *Phys. Rev. E*, **72** (2005), 1-7.

[28] V. Thomee, Galerkin Finite Element Methods for Parabolic Problems, Lecture Notes in Mathematics, **1054**, Springer-Verlag, (1997).

[29] J. Wloka, Partielle Differentialgleichungen, Teubner Stuttgart, 1982.

[30] J.-J. Xu and H.-K. Zhao, An Eulerian formulation for solving partial differential equations along a moving interface, *J. Sci. Comput.*, **19** (2003), 573-594.